

NON-THIOL 3-AMINOMETHYLBENZAMIDE INHIBITORS OF FARNESYL-PROTEIN TRANSFERASE

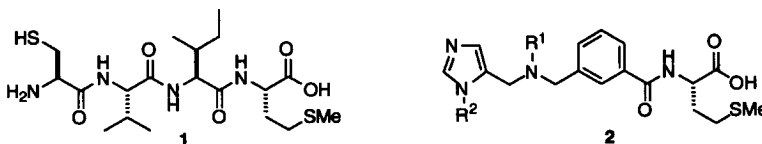
Terrence M. Ciccarone,^a Suzanne C. MacTough,^a Theresa M. Williams,^a Christopher J. Dinsmore,^{*,a}
Timothy J. O'Neill,^b Daksha Shah,^b J. Christopher Culberson,^c Kenneth S. Koblan,^b
Nancy E. Kohl,^b Jackson B. Gibbs,^b Allen I. Oliff,^b Samuel L. Graham,^a and George D. Hartman^a

*Departments of ^aMedicinal Chemistry, ^bCancer Research, and ^cMolecular Systems,
Merck Research Laboratories, West Point, PA 19486, U.S.A.*

Received 15 April 1999; accepted 27 May 1999

Abstract: The design and syntheses of non-thiol inhibitors of farnesyl-protein transferase are described. Substitutions on an imidazolylmethyl-AMBA-methionine template gave a highly potent and cell-active inhibitor.
© 1999 Elsevier Science Ltd. All rights reserved.

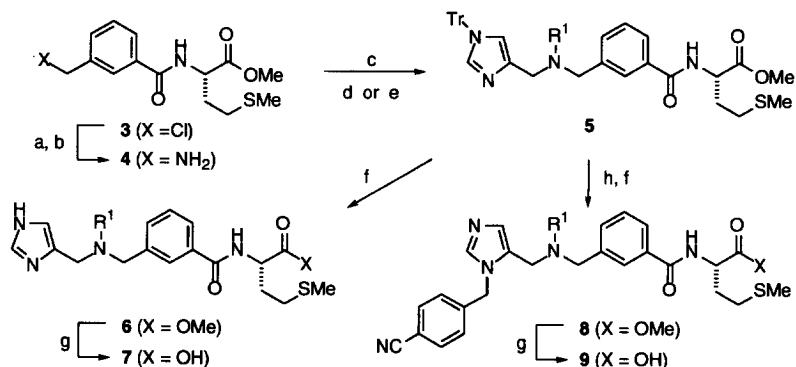
The function of the oncogene product Ras has been a topic of substantial research attention in recent years, since it plays a key part in the control of cell growth and differentiation.¹ Amino acid alterations in Ras may cause a disruption of its GTPase activity leading to failed conversion from the active GTP-bound form to the inactive GDP-bound form. Oncogenic *ras* can thereby promote unchecked cell division, and has been implicated in many forms of human cancers, including 30–50% of colon and 90% of pancreatic cancers.² The S-farnesylation of the terminal cysteine residue of Ras is required for its ability to relay extracellular growth signals to nuclear proteins by enabling association with the cell membrane.³ Thus, efforts to regulate Ras function with the goal of developing new anti-cancer therapy have focused mainly on inhibition of the zinc metalloenzyme farnesyl-protein transferase (FTase).⁴ Toward this end, studies have shown that FTase inhibitors (FTIs) can prevent protein farnesylation in cell culture and selectively inhibit *ras*-transformed cell growth,^{4,5} as well as suppress the growth of *ras*-dependent tumors in mice.⁶



Numerous inhibitors of FTase that mimic the tetrapeptide C-terminus of Ras (the Ca₁a₂X motif)⁷ have been described.⁸ Avenues toward improving the biological properties of a tetrapeptide inhibitor such as CVIM (1)^{7b} have included the use of nonpeptide surrogates for the central a₁a₂ portion, deletion of the carboxyl-containing terminus, and replacement of the cysteine moiety.⁸ Notable examples have featured the substitution of 3-aminomethylbenzoic acid (AMBA) for the central hydrophobic dipeptide,^{9,10a,b} and the use of an imidazole ring as an alternative to the cysteine thiol group.^{10c–f} In our own search for a potent non-thiol nonpeptide FTI, we have investigated imidazole-containing AMBA derivatives (e.g., 2) as surrogates for the Ca₁a₂ portion of Ca₁a₂X.¹¹ Detailed herein are the syntheses and inhibitory activity profiles of a progression of these compounds culminating in the discovery of a highly potent and cell-active non-thiol FTI.

The synthetic approach to the desired substrates (Scheme 1) began with **3**,^{10b} prepared by the acylation of L-methionine-OMe with 3-(chloromethyl)benzoyl chloride. Azidation and hydrogenation gave amine **4**.^{10b} Reductive coupling with protected imidazole-4-carboxaldehyde, followed by either a second reductive coupling or N-acylation gave **5**. Deprotection of the imidazole and ester hydrolysis provided substrates **6** and **7**, while regioselective imidazole alkylation and deprotection provided **8** and **9**, respectively.

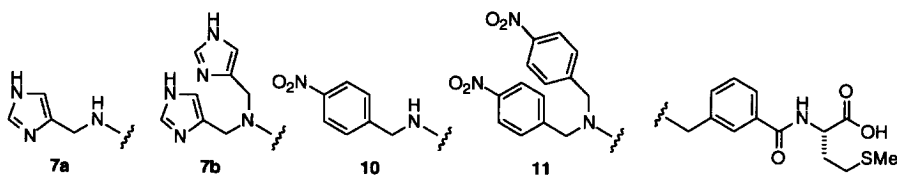
Scheme 1



(a) LiN_3 , DMSO. (b) 10% Pd/C, H_2 , MeOH. (c) Tr-imidazole-4-CHO, $\text{Na}(\text{AcO})_3\text{BH}$, 4 Å MS, $\text{ClCH}_2\text{CH}_2\text{Cl}$, 0 °C-rt. (d) aldehyde, $\text{Na}(\text{AcO})_3\text{BH}$, 4 Å MS, $\text{ClCH}_2\text{CH}_2\text{Cl}$, 0 °C-rt. (e) PhCOCl , Et_3N , CH_2Cl_2 , 0 °C (f) TFA, Et_3SiH , CH_2Cl_2 , 0 °C-rt. (g) NaOH, MeOH, H_2O . (h) 4-CN-BnBr, CH_3CN , 60 °C.

The inhibitory activities of four initial compounds (Chart 1) provided preliminary evidence for the presence of two distinct high-affinity binding regions that can be accessed from the benzylic nitrogen substituent of the AMBA-Met template. The parent imidazolymethyl derivative **7a** ($\text{IC}_{50} = 57 \mu\text{M}$) was only weakly active, but the addition of a second imidazolymethyl substituent increased the FTase potency 65-fold to a submicromolar level (**7b**, $\text{IC}_{50} = 0.87 \mu\text{M}$). This suggests the existence of a high affinity pocket for an imidazole group, and an equally significant nearby binding region. The non-imidazole compounds **10** ($\text{IC}_{50} = 80 \mu\text{M}$) and **11** ($\text{IC}_{50} = 1.6 \mu\text{M}$) suggest that the nearby binding region can accommodate neutral hydrophobic substituents, and that this region may therefore correspond to either the α_1 -side chain (of $\text{Ca}_1\alpha_2\text{X}$) binding site, or to a new domain altogether¹² (vide infra). In an in vitro counterscreen against the closely related enzyme geranylgeranyltransferase I (GGTase-I), **7b** demonstrated an IC_{50} of 17 μM , amounting to 20-fold selectivity between the prenyltransferases.

Chart 1



An investigation of the putative hydrophobic binding pocket was pursued by maintaining the imidazolymethyl substituent on AMBA constant, while varying the other (R') nitrogen substituent (Table 1). In comparison to the unsubstituted parent compound **7a**, all of the derivatized analogues were more potent inhibitors of FTase. While methylation caused only a slight increase in inhibition (**7c**), the addition of aryl groups was

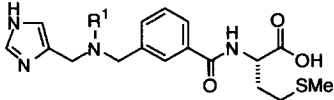
generally advantageous (**7d–7k**). In contrast to the benzamide **7d** (IC_{50} 1.7 = μ M) the benzyl derivative was significantly more potent (**7e**, IC_{50} = 255 nM), indicating either an attractive binding interaction of the basic tertiary amine with the enzyme, or a beneficial enhancement of conformational flexibility. Extension of the benzyl group to phenethyl did little to influence activity (**7f**, IC_{50} = 300 nM), but the more rigid and bulky naphthylmethyl compounds **7g** and **7h** gained five fold in potency. Substituted benzyl analogues revealed an interesting electronic influence. Relative to **7e**, the electron rich 4-methoxybenzyl analogue **7i** was slightly less potent (IC_{50} = 355 nM). However, the electron deficient 4-nitro compound **7j** conferred almost ten fold enhancement of inhibitory activity (IC_{50} = 27 nM). The nitrile **7k** was even more potent, exhibiting the best activity in the series (IC_{50} 12 nM), and demonstrating a 4800-fold gain relative to the parent unsubstituted imidazolylmethyl-AMBA **7a**. The influence of the 4-cyanobenzyl group on GGTase-I inhibition was less significant than for FTase; whereas the modification **7b**→**7k** caused a 72-fold improvement in FTase activity, only three fold enhancement of activity against GGTase-I was realized (**7k** IC_{50} GGTase-I = 6.2 μ M). Thus, substitution on the AMBA nitrogen with a cyanobenzyl group gave the highly potent **7k** with 300-fold selectivity for FTase over GGTase-I.

The results in Table 1 are in agreement with a previous report¹²

which indicated the presence of a novel high-affinity aromatic binding pocket in FTase, by demonstrating that replacement of a cysteine residue with *para*-substituted benzyl thioethers in pseudotetrapeptides gave highly potent FTIs. In fact, the aromatic substituent effects observed herein closely parallel those of the earlier work (IC_{50} **7i**(MeO) > **7j**(NO₂) > **7k**(CN)). Because the imidazole and substituted aromatic rings are linked through only a three atom distance in the AMBA FTIs, the close spatial proximity of their respective binding pockets in the FTase active site is corroborated.

Because of the spatial proximity of the nitrogen atoms bearing substituents R¹ and R² in **2**, it seemed plausible that the benzylic nitrogen substituent (R¹) could be migrated to the proximal imidazole nitrogen without substantially affecting potency. Thus, using the nitrile **7k** as a starting point for analysis of structure-activity relationships, a series of 1-(4-cyanobenzyl)-5-imidazolylmethyl¹³ derivatives was evaluated (Table 2). In comparison to R¹-cyanobenzyl compound **7k**, the R²-cyanobenzyl regioisomer **9a** was only two fold less potent (IC_{50} = 23 nM), in support of the notion that the R¹ and R² substituents might probe the same region in the FTase active site. However, in the event that distinctly different hydrophobic binding regions are accessed by the R¹ and R² substituents, the reinstallation of an R¹ group in **9a** would increase the inhibitory activity. To investigate this possibility, R¹-R² disubstituted analogues were prepared. Gratifyingly, the *n*-butyl derivative regained potency by two fold (**9b**, IC_{50} = 14 nM), and the bis(4-cyanobenzyl) **9c** was significantly more active (IC_{50} = 0.41 nM). The

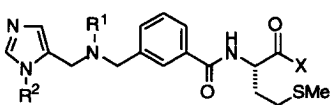
Table 1



compd	R	IC_{50} (nM) ^a
7a	H	57,600
7c	Me	12,000
7d	PhCO	1,750
7e	PhCH ₂	255
7f	PhCH ₂ CH ₂	300
7g	1-naphthyl-CH ₂	58
7h	2-naphthyl-CH ₂	55
7i	4-(MeO)-benzyl	355
7j	4-(NO ₂)-benzyl	27
7k	4-(CN)-benzyl	12

(a) Concentration of compound required to reduce the FTase-catalyzed incorporation of [³H]FPP into recombinant Ha-Ras by 50%. The assay used enzyme purified from bovine brain at a concentration of ca. 1 nM, as described in ref 5a.

Table 2



compd	R ¹	R ²	X	IC ₅₀ (nM) ^a	Soft Agar MIC (μM) ^b		
					H- <i>ras</i>	<i>raf</i>	CTE (μM) ^c
7k	4-(CN)benzyl	H	OH	12	-	-	-
9a	H	4-(CN)benzyl	OH	23	-	-	-
9b	<i>n</i> -Bu	4-(CN)benzyl	OH	14	-	-	-
9c	4-(CN)benzyl	4-(CN)benzyl	OH	0.41	-	-	-
6k	4-(CN)benzyl	H	OMe	1,075	10	>10	≥50
8a	H	4-(CN)benzyl	OMe	260	10	>10	25
8b	<i>n</i> -Bu	4-(CN)benzyl	OMe	183	>10	>10	25
8c	4-(CN)benzyl	4-(CN)benzyl	OMe	5	≤1	>10	25

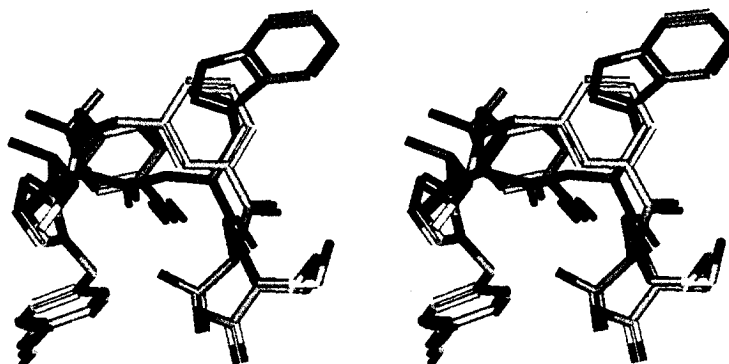
(a) See corresponding footnote in Table 1. For IC₅₀ < 1 nM, enzyme concentration was 10 pM in the assay. (b) Minimum inhibitory concentration (MIC) required to achieve a reduction in size and number of colonies of RAT1 v-Ha-*ras* (Ras2B) or RAT1 v-*raf*-(Raf1a1) transformed cells in soft agar relative to vehicle-treated control. Assay conditions are described in ref 5b. (c) Highest nontoxic concentration (≥90% cell survival) for cultured RAT1 cells as assessed by viable staining with MTT.

structural comparison of the subnanomolar FTI **9c** with the 30- to 50-fold less potent mono(4-cyanobenzyl) isomers **7k** and **9a** implies the existence of two high-affinity binding sites adjacent to the putative zinc binding position.

With the highly potent FTIs **7k** and **9a–c** in hand, an evaluation of in vivo cell activity was warranted. An effective method for enhancing cell penetration of carboxyl-containing CaaX peptidomimetics is to mask the polar C-terminus as an ester prodrug.⁸ Accordingly, the corresponding methyl esters **6k** and **8a–c** were examined in cell-based assays. In an assay that measures inhibition of cell growth in soft agar, the mono(4-cyanobenzyl) FTIs **6k**, **8a**, and **8b** failed to reduce the size and number of colonies of Ha-*ras* transformed RAT1 cells at concentrations below 10 μM. Moreover, inhibition of *ras*-independent *raf*-transformed cell growth may have occurred at similar minimum inhibitory concentrations (MICs > 10 μM), and the window between growth inhibition and cellular cytotoxicity (CTE ≥ 25 μM) was narrow for the three compounds. Thus, although the active acid metabolites of **6k**, **8a**, and **8b** possess good inhibitory activity against FTase in vitro, the esters exhibited relatively poor cell activity, and no conclusion could be drawn with regard to their mechanism of cell growth inhibition.

In contrast to the mono(4-cyanobenzyl) compounds, the prodrugged bis(4-cyanobenzyl) FTI **8c** was found to be both potent and selective in cell culture (Table 2). Inhibition of Ha-*ras* transformed cell growth was observed at a remarkably low concentration in soft agar (MIC ≤ 1 μM). Moreover, in a protein processing assay,^{5c} **8c** inhibited the post-translational prenylation of Ha-Ras protein in cultured NIH3T3 cells with an IC₅₀ ~5 μM. In the control studies to determine selectivity, *raf*-transformed cell growth was uninhibited below 10 μM concentration in soft agar, and even higher concentration of **8c** was required to engender cellular cytotoxicity in RAT1 cells (CTE 25 μM). Since the primary goal in the chemotherapeutic approach to cancer treatment is the control of cancer cell growth without toxicity to normal cells, it is notable that activity of compound **8c** in soft agar

Figure 1 Best-fit superposition (cross-eyed stereoview) of compound **9c** (gray) and the FTase-bound conformation of CVWM (green) as determined by ^1H NMR transferred NOE spectroscopy (ref 15b). Hydrogens have been omitted for clarity.



enabled the reversal of anchorage independent growth, one of the phenotypic changes typical of cancerous cells.

The three-dimensional structure of an FTI such as **9c** bound in the farnesyltransferase enzyme active site would be useful information for the design of related compounds with improved biological and pharmacological properties. The crystal structure of rat FTase¹⁴ bound to an FPP analogue and the tetrapeptide *N*-Ac-CVI(seleno)M was recently determined, supporting an extended conformation hypothesis for the bound $\text{Ca}_1\text{a}_2\text{X}$ inhibitor.^{14b} Earlier structural studies using ^1H NMR transferred NOE (TRNOE) spectroscopy,¹⁵ in conjunction with the crystallographic data, suggest the possibility of alternate CaaX binding modes. In one of these,^{15b} the tetrapeptide CVWM was found to adopt a conformation most closely approximating a type III β -turn, featuring a proximal spatial relationship between the cysteine thiol and terminal carboxylate groups. A comparison of CaaX mimics to either of the FTase-bound conformational models is instructive; overlay of energy-minimized **9c** onto the TRNOE-derived CVWM structure (Figure 1) provides one possible hypothesis for its FTase-bound conformation, and supports some of the observed SAR.^{16,17} In the overlapped structures, the 3-aminomethylbenzamide aligns itself with the peptide backbone to provide a scaffold for the superposition of the key terminal binding groups, with the aromatic ring projecting into the α_2 -hydrophobic (tryptophan side-chain binding) region. In addition to overlap of the methionine residues, the putative zinc-binding imidazole and cysteine thiol groups lie closely in register. The (R^1) 4-cyanobenzyl group is projected toward the α_1 -hydrophobic (valine side-chain binding) pocket, and the terminal (R^2) 4-cyanobenzyl group attached to imidazole reaches into an undefined high-affinity aromatic binding region.¹² Although the model presents an explanation for the loss in potency on deletion of either of the cyanobenzyl substituents in **9c**, the exact position of the high-affinity (R^2) aromatic binding pocket as well as the origin of aryl substituent effects (Table 1) remain unexplained.

Compounds based on the imidazolylmethyl-AMBA-methionine template are highly potent inhibitors of farnesyltransferase. The bis(4-cyanobenzyl) FTI **9c** was found to have subnanomolar potency in vitro, and the corresponding methyl ester prodrug **8c** is a highly selective and potent inhibitor of *ras*-transformed cell growth and Ras processing in cell culture.

Acknowledgment: We are grateful to G. M. Smith, K. D. Anderson, P. A. Ciecko, M. M. Zrada, H. G. Ramjit, and A. B. Coddington for analytical support, and to J. M. Hartzell for manuscript assistance.

References and Notes

- (a) Barbacid, M. *Annu. Rev. Biochem.* **1987**, *56*, 779. (b) Kato, K.; Cox, A. D.; Hisaka, M. M.; Graham, S. M.; Buss, J. E.; Der, C. J. *Proc. Natl. Acad. Sci. U.S.A.* **1992**, *89*, 6403.
- Rodenhuis, S. *Semin. Cancer Biol.* **1992**, *3*, 241.
- (a) Casey, P. J.; Solski, P. J.; Der, C. J.; Buss, J. E. *Proc. Natl. Acad. Sci. U.S.A.* **1989**, *86*, 8323. (b) Kato, K.; Cox, A. D.; Hisaka, M. M.; Graham, S. M.; Buss, J. E.; Der, C. J. *Proc. Natl. Acad. Sci. U.S.A.* **1992**, *89*, 6403.
- (a) Gibbs, J. B. *Cell* **1991**, *65*, 1. (b) Gibbs, J. B.; Oliff, A. I.; Kohl, N. E. *Cell* **1994**, *77*, 175.
- (a) Moores, S. L.; Shaber, M. D.; Mosser, S. D.; Rands, E.; O'Hara, M. B.; Garsky, V. M.; Marshall, M. S.; Pompliano, D. L.; Gibbs, J. B. *J. Biol. Chem.* **1991**, *266*, 14603. (b) Kohl, N. E.; Mosser, S. D.; deSolms, S. J.; Giuliani, E. A.; Pompliano, D. L.; Graham, S. L.; Smith, R. L.; Scolnick, E. M.; Oliff, A. I.; Gibbs, J. B. *Science* **1993**, *260*, 1934. (c) Gibbs, J. B.; Pompliano, D. L.; Mosser, S. D.; Rands, E.; Lingham, R. B.; Singh, S. B.; Scolnick, E. M.; Kohl, N. E.; Oliff, A. I. *J. Biol. Chem.* **1993**, *251*, 7617.
- (a) Kohl, N. E.; Wilson, F. R.; Mosser, S. D.; Giuliani, E. A.; deSolms, S. J.; Conner, M. W.; Anthony, N. J.; Holt, W. J.; Gomez, R. P.; Lee, T.-J.; Smith, R. L.; Graham, S. L.; Hartman, G. D.; Gibbs, J. B.; Oliff, A. I. *Proc. Natl. Acad. Sci. U.S.A.* **1994**, *91*, 9141. (b) Kohl, N. E.; Omer, C. A.; Conner, M. W.; Anthony, N. J.; Davide, J. P.; deSolms, S. J.; Giuliani, E. A.; Gomez, R. P.; Graham, S. L.; Hamilton, K.; Handt, L. K.; Hartman, G. D.; Koblan, K. S.; Kral, A. M.; Miller, P. J.; Mosser, S. D.; O'Neill, T. J.; Shaber, M. D.; Gibbs, J. B.; Oliff, A. I. *Nature Med.* **1995**, *1*, 792.
- (a) CaaX; 'C' = cysteine, 'a' = any aliphatic amino acid, 'X' = a prenylation specificity residue. (b) Reiss, Y.; Goldstein, J. L.; Seabra, M. C.; Casey, P. J.; Brown, M. S.; *Cell* **1990**, *62*, 81.
- Recent reviews: (a) Graham, S. L. *Exp. Opin. Ther. Patents* **1995**, *5*, 1269. (b) Graham, S. L.; Williams, T. M. *Exp. Opin. Ther. Patents* **1996**, *6*, 1295. (c) Sebt, S. M.; Hamilton, A. D. *Pharmacol. Ther.* **1997**, *74*, 103. (d) Leonard, D. M. *J. Med. Chem.* **1997**, *40*, 2971. (e) Williams, T. M. *Exp. Opin. Ther. Patents* **1998**, *8*, 553.
- 3-Aminomethylbenzoic acid as a dipeptide mimetic: Stewart, F. H. C. *Aust. J. Chem.* **1983**, *36*, 2511.
- (a) Nigam, M.; Seong, C.-M.; Qian, Y.; Hamilton, A. D.; Sebt, S. M. *J. Biol. Chem.* **1993**, *268*, 20695. (b) Qian, Y.; Blaskovich, M. A.; Saleem, M.; Seong, C.-M.; Wathen, S. P.; Hamilton, A. D.; Sebt, S. M. *J. Biol. Chem.* **1994**, *269*, 12410. (c) Leftheris, K.; Kline, T.; Natarajan, S.; Devirgilio, M. K.; Cho, M. H.; Pluscec, J.; Ricca, C.; Robinson, B. R.; Seizinger, B.; Manne, V.; Meyers, C. A. *Bioorg. Med. Chem. Lett.* **1994**, *4*, 887. (d) Hunt, J. T.; Lee, V. G.; Leftheris, K.; Seizinger, B.; Carboni, J.; Mabus, J.; Ricca, C.; Yan, N.; Manne, V. *J. Med. Chem.* **1996**, *39*, 353. (e) Leonard, D. M.; Shuler, K. R.; Poulter, C. J.; Eaton, S. R.; Sawyer, T. K.; Hodges, J. C.; Su, T.-Z.; Scholten, J. D.; Gowan, R. C.; Sebolt-Leopold, J. S.; Doherty, A. M. *J. Med. Chem.* **1997**, *40*, 192. (f) Kaminski, J. J.; Rane, D. F.; Snow, M. E.; Weber, L.; Rothofsky, M. L.; Anderson, S. D.; Lin, S. L. *J. Med. Chem.* **1997**, *40*, 4103.
- A related study has led to pyridyl-substituted FTIs: Augeri, D. J.; O'Connor, S. J.; Janowick, D.; Szczepankiewicz, B.; Sullivan, G.; Larsen, J.; Kalvin, D.; Cohen, J.; Devine, E.; Zhang, H.; Cherian, S.; Saeed, B.; Ng, S.-C.; Rosenberg, S. *J. Med. Chem.* **1998**, *41*, 4288.
- Breslin, M. J.; deSolms, S. J.; Giuliani, E. A.; Stokker, G. E.; Graham, S. L.; Pompliano, D. L.; Mosser, S. D.; Hamilton, K. A.; Hutchinson, J. H. *Bioorg. Med. Chem. Lett.* **1998**, *8*, 3311.
- Anthony, N. J.; Gomez, R. P.; Schaber, M. D.; Mosser, S. D.; Hamilton, K. A.; O'Neill, T. J.; Koblan, K. S.; Graham, S. L.; Hartman, G. D.; Shah, D.; Rands, E.; Kohl, N. E.; Gibbs, J. B.; Oliff, A. I. *J. Med. Chem.* In press.
- (a) Park, H.-W.; Boduluri, S. R.; Moomaw, J. F.; Casey, P. J.; Beese, L. S. *Science* **1997**, *275*, 1800. (b) Strickland, C. L.; Windsor, W. T.; Syto, R.; Wang, L.; Bond, R.; Wu, Z.; Schwartz, J.; Le, H. V.; Beese, L. S.; Weber, P. C. *Biochemistry* **1998**, *37*, 16601.
- (a) Stradley, S. J.; Rizo, J.; Gierasch, L. M. *Biochemistry* **1993**, *32*, 12586. (b) Koblan, K. S.; Culbertson, J. C.; deSolms, S. J.; Giuliani, E. A.; Mosser, S. J.; Omer, C. A.; Pitzenberger, S. M.; Bogusky, M. J. *Prot. Sci.* **1995**, *4*, 681.
- (a) Conformations were generated using metric matrix distance geometry algorithm JG (S. Kearsley, Merck & Co., Inc., unpublished). Conformations were subjected to energy-minimization within MacroModel^{16b} using the MM2* force field. Overlay of generated energy minimized conformations was done using SQ.^{16c} (b) Mohamadi, F.; Richards, N. G. J.; Guida, W. C.; Liskamp, R.; Caufield, C.; Chang, G.; Hendrickson, T.; Still, W. C. *J. Comput. Chem.* **1990**, *11*, 440. (c) Miller, M.; Sheridan, R. P.; Kearsley, S. K. *J. Med. Chem.* **1999**, *42*, 1505.
- Although comparisons to both turned and extended conformational models warrant consideration, only the turned model is illustrated as an example. Qualitatively, the relationships between turned **9c** and turned CVWM^{15b} are the same as between extended **9c** and extended *N*-Ac-CVI(seleno)M.^{14b}